

Solid state laser applications in photovoltaics manufacturing

Corey Dunsky* and Finlay Colville
Coherent Inc., 5100 Patrick Henry Drive, Santa Clara, CA 95054

ABSTRACT

Photovoltaic energy conversion devices are on a rapidly accelerating growth path driven by increasing government and societal pressure to use renewable energy as part of an overall strategy to address global warming attributed to greenhouse gas emissions. Initially supported in several countries by generous tax subsidies, solar cell manufacturers are relentlessly pushing the performance/cost ratio of these devices in a quest to reach true cost parity with grid electricity. Clearly this eventual goal will result in further acceleration in the overall market growth. Silicon wafer based solar cells are currently the mainstay of solar end-user installations with a cost up to three times grid electricity. But next-generation technology in the form of thin-film devices promises streamlined, high-volume manufacturing and greatly reduced silicon consumption, resulting in dramatically lower per unit fabrication costs. Notwithstanding the modest conversion efficiency of thin-film devices compared to wafered silicon products (around 6-10% versus 15-20%), this cost reduction is driving existing and start-up solar manufacturers to switch to thin-film production. A key aspect of these devices is patterning large panels to create a monolithic array of series-interconnected cells to form a low current, high voltage module. This patterning is accomplished in three critical scribing processes called P1, P2, and P3. Lasers are the technology of choice for these processes, delivering the desired combination of high throughput and narrow, clean scribes. This paper examines these processes and discusses the optimization of industrial lasers to meet their specific needs.

Keywords: Thin-film solar cells, solar panels, lasers, scribing, ablation, conversion efficiency, photovoltaics

1. THIN-FILM PHOTOVOLTAIC ARCHITECTURE

Three different semiconductor materials are at various stages of development for use in thin-film solar cells: amorphous silicon (a-Si), cadmium telluride (CdTe) and copper indium diselenide (CIS) or copper indium gallium diselenide (CIGS). As of 2006, these three thin-film systems comprised only 6 percent of the rapidly-expanding worldwide solar cell production, with the remainder captured by bulk silicon technologies (wafered cells, ribbon cells, and a-Si/wafered silicon hybrid cells).¹ Thin-film cell production, however, is forecast to experience significantly higher growth rates in the next three to five years than that of bulk-silicon cells. In 2006, a-Si cells were 4% of the worldwide total, with CdTe and CIS/CIGS at 1.8% and 0.3%, respectively.²

Due to the toxicity of cadmium, CdTe technology has until recently suffered from a public perception of possible environmental and human-health hazards. Though the final product has been conclusively shown to be safe, the manufacturing process must contain the cadmium during the deposition and laser scribing processes; consequently few manufacturers have developed the specialized equipment required. In 2006, one manufacturer was responsible for almost 90% of the total worldwide CdTe module production. That manufacturer, however, has recently reported manufacturing costs that indicate CdTe is currently the least expensive PV technology to manufacture; other thin-film manufacturers have announced CdTe pilot production plans suggesting an increase in the number of companies pursuing this technology. CIS/CIGS is presently considered a promising but “on-the-horizon” material, with volume production pushed out from 2007 to the 2008-2010 timeframe.

Today and for the next few years, therefore, a-Si will account for the lion’s share of the thin-film photovoltaic (TFPV) market: a recent projection³ estimates that the six-year (2006-2012) compound annual growth rate for a-Si TFPV production will range between 47 and 65 percent. Therefore, we focus our discussion here on the specifics of the laser-based production steps for a-Si modules, though the same basic scheme applies to CdTe and CIS/CIGS, as well.

* corey.dunsky@coherent.com: phone 1-408-764-4678; fax 1-408-764-4825; www.coherent.com

The most common format for a-Si (and CdTe) is single-junction and is based on a glass superstrate architecture as shown in schematic cross-section in Figure 1. As implied by their very name – “thin-film” - these devices consist of multiple thin layers of material deposited on sheet glass. The term superstrate (as opposed to substrate) is used as these are back-side devices in which sunlight enters through the support glass.

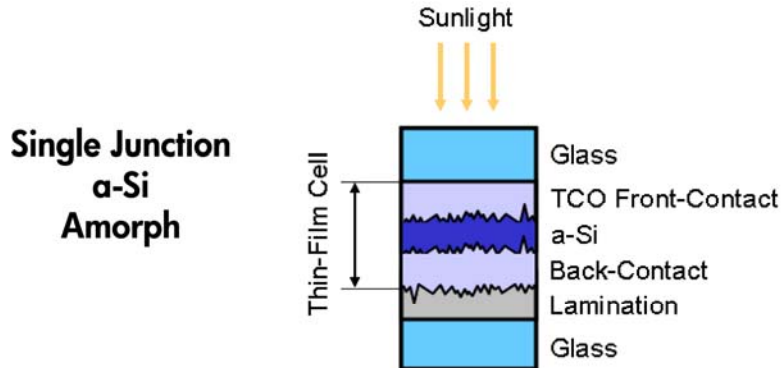


Fig. 1. Thin-film solar cells based on a-Si use a glass superstrate architecture in which sunlight enters through the support glass. The rear surface is sealed with a laminated sheet of glass.

Each panel starts off as a sheet of glass with a typical thickness of 3mm or 1/8 inch. Various layers of conductor and semiconductor are then vapor deposited across the entire area of the panel. The first layer is a TCO (transparent conductive oxide) a few hundred nanometers thick which forms the collector electrode. The second film is a pair of *p* and *n* silicon layers that form the active *p-n* junction. This a-Si has to be thick enough to absorb most of the incident sunlight, but not so thick that charge carrier recombination predominates over charge collection at the electrodes. Typical optimum overall thickness for this silicon layer is 2-3 microns. The final film is metal (Al or Mo) that forms the rear electrodes. Typical thickness of the metal layer is a few hundred nanometers. The panel is then sealed to protect against physical and environmental damage by laminating with a second sheet of glass.

The size of these panels continues to increase in order to maximize one key advantage of thin-film devices, namely low-cost, high-volume fabrication of large active-area panels. The Solar industry today mainly manufacturers Gen 5 panel sizes, with dimensions 1100 x 1300 mm. But the upcoming Gen 8.5 will move to 2200 x 2600 mm panels. These large glass panels are typically sub-divided into a large number (up to 165 for Gen 5) of individual solar cells during ‘cell-definition’ scribing steps (P1, P2, P3) which also define the electrical interconnects for adjacent cells (see Figure 2). Specifically, this cell definition creates low-current active ‘strips’ that are connected in series in order to produce large additive voltages from the overall panel. These narrow strips span the entire width of the panel (i.e. 1-2 m) but are only 5-10 mm in the other dimension so as to limit the current. With this architecture, a typical finished panel may have a rated power at the 100 W level (Gen 5), with currents below 10 A. This ‘cell-definition’ is also referred to as patterning.

2. LASER SCRIBING – P1, P2, P3

As shown in Figure 3, the production sequence dictates that each of the three (TCO, a-Si, Al) vapor deposition steps is followed by a scribing step. The three laser scribing processes are well-developed and have been described in detail elsewhere.^{4,6} The purpose of P1 is to completely cut through the TCO, thereby defining one edge of each individual cell. In Fig. 3, the P1 scribe defines the right-hand edge of each cell. P2 must cut through the a-Si but leave the TCO intact, so as to form the pathway for series interconnection between adjacent cells. P3, the final patterning step, needs to cut through both the a-Si and the overlaying metal, again leaving the TCO intact, and defines the left-hand edge of each cell (Fig. 3).

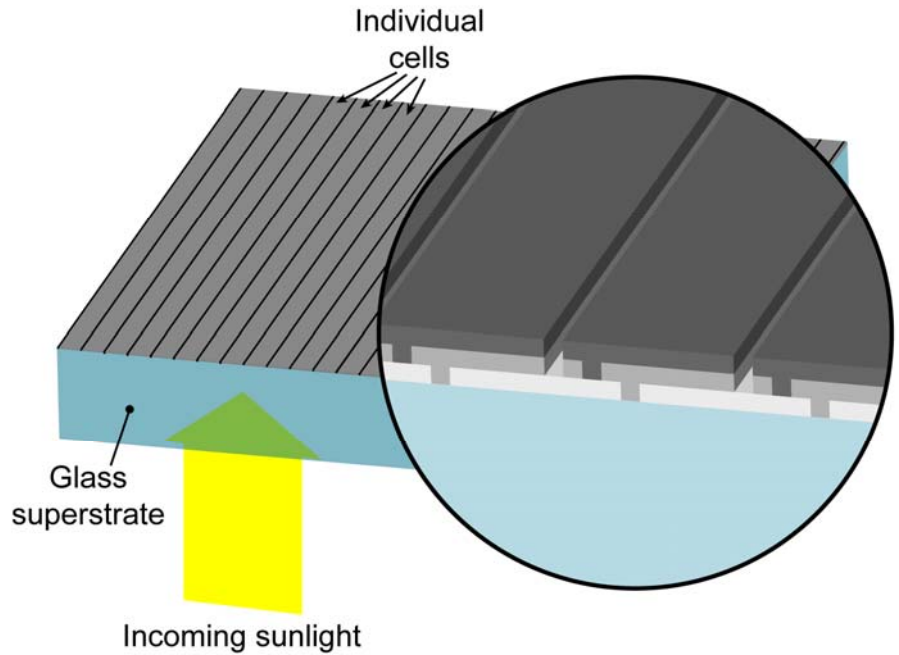


Fig. 2. Thin film solar panels are fabricated as large monolithic sheets which are then patterned into a large number of individual strip-shaped solar cells, electrically connected in series.

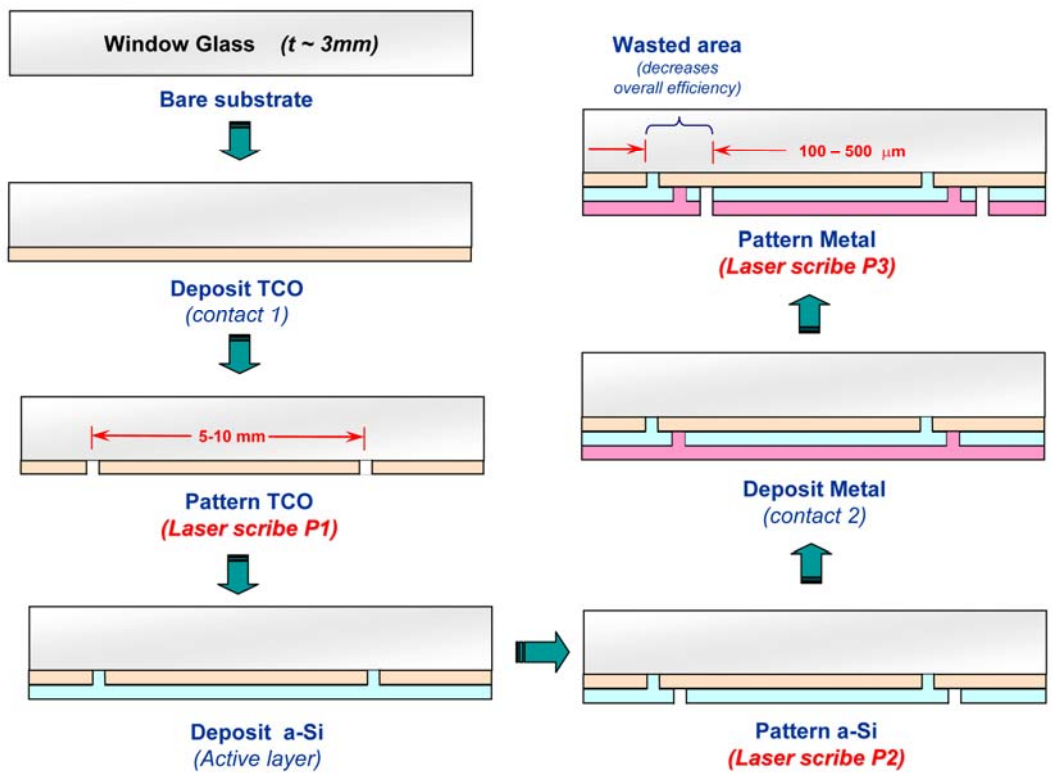


Fig. 3. After each of the thin film layers are deposited, the film must be patterned using narrow scribes.

At this early phase of market adoption, thin-film solar panels are inherently commodity (low value-added) products, in marked contrast to their cousins in the flat panel display industry. This, combined with the need to reduce overall installed costs to achieve cost parity with grid power, maintains a constant economic pressure to drive down manufacturing costs. Yet manufacturing methods must also maximize the modest conversion efficiency of the final product, since the key cost metric is Watts/Dollar (\$/W). With this overriding constraint, laser micromachining is the only practical method possessing the potential to create these scribes with the material and depth selectivity just outlined. Moreover, lasers can deliver the requisite combination of edge quality, process repeatability, high throughput and high yield in an application that is cost-driven, yet performance sensitive. Simply stated, there is no practical mechanical alternative. Lithographic methods could achieve the required results, but, in practice, these are slow and involve too much wet chemistry to be economically viable.

2.1. Achieving Material Selectivity Through Laser Wavelength Choice

Laser machining is now well-established in a wide range of cutting and scribing applications involving a diverse range of materials. An equally diverse range of laser technologies, with CW or pulsed (nanosecond and sub-nanosecond) output, and a broad range of wavelengths, support these processes. Q-switched DPSS (diode pumped solid state) lasers are the tools of choice for P1, P2 and P3 scribes in part because of their solid state reliability, compact packaging and superior beam quality. Just as important, careful selection of the laser wavelength automatically provides material selectivity, eliminating the cost and complexity of implementing active depth control. In volume production, these scribing processes are performed through the front side glass since this geometry allows the P2 and P3 scribes to be rapidly created via a “micro-explosive” mechanism. So, P1 needs a laser wavelength that transmits through glass but is strongly absorbed by the TCO. This precludes the use of mid-infrared or deep-UV lasers which would be absorbed by the glass. It also eliminates the use of visible lasers which would not be absorbed well by the TCO – which, by very definition, is transparent at visible wavelengths! The near infrared (1.06 micron) fundamental of a DPSS laser is almost perfect for this application; even several watts of laser power transmits through the glass superstrate with no damage, yet this wavelength is strongly absorbed by the TCO layer. And since this TCO layer is very thin (a few hundred nanometers) it can be completely ablated in a single pass at this power level.

P2 (and P3) scribing involves removal of much more material than for P1, owing to the silicon layer's greater thickness. With conventional ablation, removing more material requires that the laser power be increased by a corresponding amount. But a novel “micro-explosive” liftoff process allows this to be accomplished at high speed, without the use of high laser power which could damage the glass or TCO, as well as increase capital costs and potentially limit scribe spatial resolution. (This material removal process is based on a well-established technique that uses 308 nm Excimer lasers for high-speed production of high resolution PCBs and flex circuits for cost sensitive applications such as disposable medical sensors). In this case, P2 uses a frequency-doubled DPSS laser with 532 nm output. The green beam passes through the glass and the TCO. In particular, the weak absorption of TCO at 532 nm allows it to transmit at the 1 watt power level without sustaining any damage. Since silicon absorbs this green laser light very strongly, much of the laser pulse energy is therefore deposited at the TCO-silicon interface. This cleanly and completely blows off the overlying silicon layer, at much lower power levels than would be needed for either photo-thermal or photo-chemical ablation processes. P3 uses exactly the same process; the thin film of metal is carried away with the underlying silicon. Because this is a binary-threshold process, producing clean edges dictates the use of a masked beam rather than a focused beam. In practice, a circular mask is used to aperture the central portion of the Gaussian laser beam so that the intensity exceeds the process threshold across the entire apertured beam. Figure 4 schematically summarizes these three scribing processes.

3. KEY SCRIBING REQUIREMENTS

In order to define optimum laser output characteristics for each of these scribes, it is first necessary to examine the critical requirements from a production viewpoint. Compared to wafered-silicon PV cells, the main advantage of thin-film solar panels is to lower costs, while tolerating lower conversion efficiency. So for any fabrication step, the key metrics are lowering per area production costs while maintaining/maximizing efficiency. As with any type of high volume, commodity manufacturing, yield and throughput are critical to lowering overall scribing costs. (At this early

stage, manufacturers are understandably reticent to discuss target yields, but based on similar processes in FPD fabrication, yields in excess of 95% should be achievable in three to five years⁷).

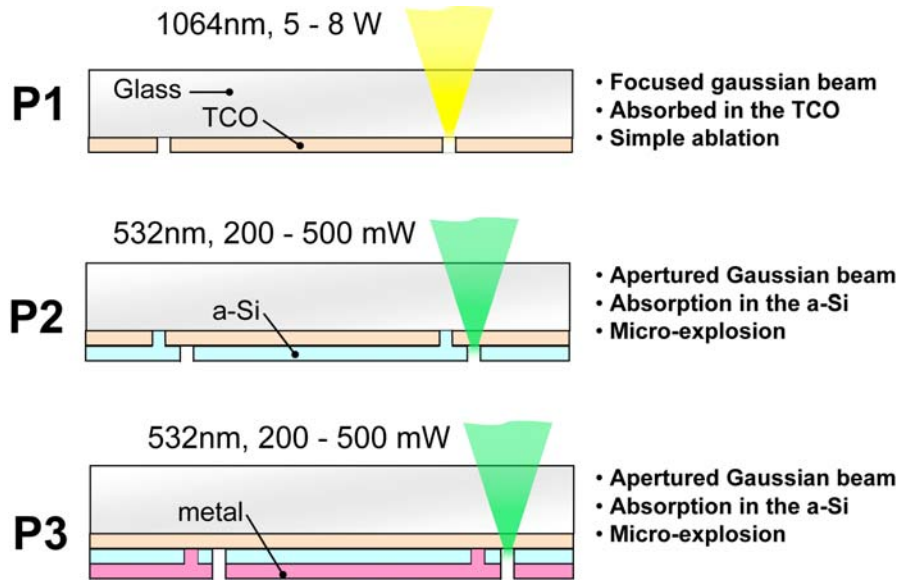


Fig. 4. Side view showing how the three completed scribes define individual solar cells and series interconnects.

3.1. Cut Integrity – Zero Defects

There are two factors that can lower yields: a defective process resulting in scrap product, or an equipment breakdown resulting in no product, i.e., unscheduled downtime. How can scrap product arise? For all three scribes, cut integrity is obviously very important, in terms of both cut depth and continuity. Specifically, the P1 scribe must cut completely through the full depth of the transparent oxide layer. This cut defines and isolates the individual cells, so it must be complete across the entire width of the panel to give an effective resistance of tens of megaohms. Any defects in this can lower the resistance and even potentially completely short that cell out of the series circuit. Figure 5 shows recent high-speed P1 scribing results.

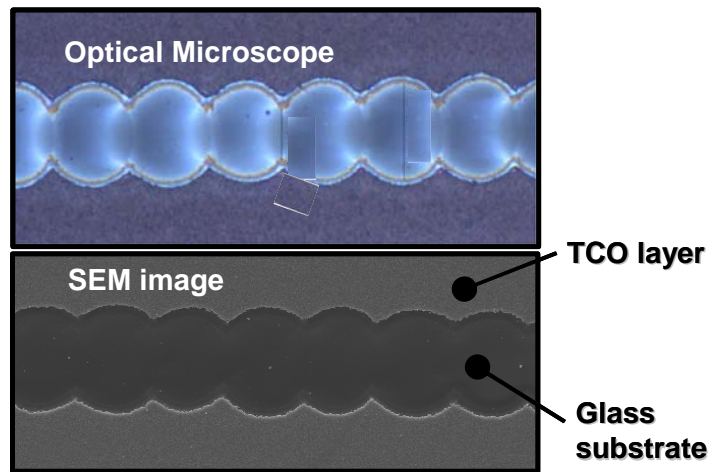


Fig. 5. P1 scribes (1064nm wavelength, through the glass, TCO layer removed)

The integrity of the P2 scribe is also critical, serving to form the series interconnects between cells. After the scribe, any active-layer (a-Si) material remaining over the TCO layer will impose contact resistance in the TCO-to-metal interconnection, resulting in parasitic losses and decreased electrical power output of the module. Figure 6 shows recent high-speed P2 scribing results.

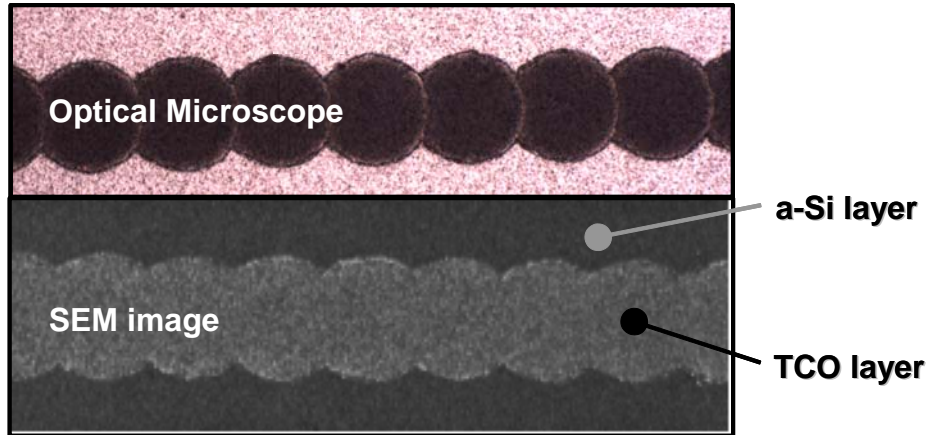


Fig. 6. P2 scribes (532nm wavelength, through the glass, a-Si layer removed)

The integrity and continuity of P3 is as critical as P1. Cutting through both the backside electrodes and semiconductor layers, P3 again serves to define and isolate adjacent cells. Defects can allow a short, essentially eliminating a cell as an active element in the current series. Figure 7 shows recent high-speed P3 scribing results.

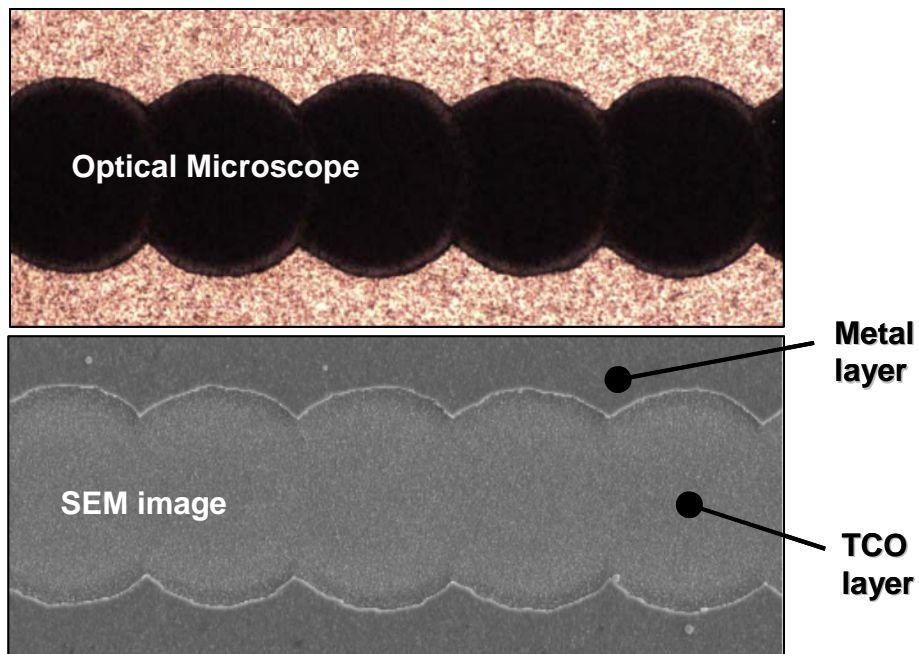


Fig. 7. P3 scribes (532nm wavelength, through the glass, a-Si and metal layers removed)

3.2. Cut Resolution and Linearity

Cut resolution and precise spatial location are also important to both yield (i.e. overall fabrication cost) and conversion efficiency. Referring back to figure 3, the area between P1 and P3 is a non-active (i.e. wasted or 'dead') area. This area is a fraction of a millimeter in width; scribe lines are currently 50-100 microns in width with an offset separation between P1 and P3 of hundreds of microns. But given that each cell typically has a total width of less than 10 mm, and also the importance of maximizing the inherently low (6-10%) conversion efficiency, it's vital to further minimize this already small inter-scribe area. This means narrow scribes that are placed as close to each other as possible. Of course, this scribe narrowing must be accomplished without increasing scribe defects. (Gen 8.5 is projected to decrease linewidths to the 20-50 micron range.) In addition, the use of closer spaced scribes requires very straight cuts that don't wander out of alignment, or else scrap product can result – this also presents significant challenges for the scan optics which must follow the continuous motion of the panel through the laser scribing tool.

3.3. Edge Quality

Cut quality is another important consideration, specifically in terms of edge roughness and microcracking. One of the principal factors limiting conversion efficiency is recombination of charge carriers inherent in this type of device. Some recombination mechanisms are dependent on surface area and local band defects due to microcracks and/or other sub-surface thermal damage caused during scribing. So overall conversion is maximized by creating scribes with smooth edges and no recast debris (for minimum surface area and defects), as well as scribes with minimized peripheral thermal damage. In laser micromachining, this peripheral damage is commonly referred to as the HAZ (heat affected zone).

In Figs. 5-7, it is evident that at the nominal process conditions, a low pulse-to-pulse overlap is used. Intensive process-characterization by Haas, et.al.⁸ has shown that such low overlap is desired in order to avoid peeling of the active (a-Si) and back-contact (metal) layers induced by the laser pulses. Particularly for the P2 step, peeling or ridges of re-cast material at the edges of the scribe can lead to failure of the metal layer to properly adhere and can also create recombination sites. Low overlap mitigates that problem; typically, a pulse overlap of about 25% is used in all three process steps.

3.4. Speed and Throughput

Throughput is the other critical parameter impacting overall fabrication costs. Each generation of thin-film devices is scaling to ever larger area panels in order to drive down unit costs. Ideally, this scaling should have no negative impact on process speed as defined by TAKT time – the time a panel spends at each station in the continuous-flow production line. Laser scribing certainly should not be the limiting factor determining TAKT time. As Gen 8.5 devices are in their infancy, specific TAKT times are yet to be established accurately, but these are widely considered to be in the range of several minutes, which means scribe rates have to be in the range 2 meters/second, because each panel involves well over 100 meters of scribing for each of P1, P2 and P3.

4. OPTIMIZED LASER OUTPUT PARAMETERS

Based on established Nd:YVO₄ laser technology, our company has developed a series of near-IR and green lasers fully optimized to meet the process requirements of P1, P2 and P3 scribing. Some specific requirements and characteristics of the laser source are described next.

4.1. Modest Power with High Pulse Repetition Rates

Other than wavelength, the most important laser characteristics for high-volume, precision machining applications are average power and pulse repetition rate. These are particularly important when scaling up a high volume application, as in the Gen 5 to Gen 8.5 transition, as they ultimately determine the maximum processing speed and hence throughput. As previously discussed, in the case of all three scribes, up to hundreds meters of scribing must be performed in a few minutes at most. Even with novel high-speed scanning systems, this means that multiple laser beams must be used in each of the scribing stations with a target scan rate of 2 meter/sec for Gen 8.5. Because of this use of multiple lasers,

the average power requirement for single pass scribing is quite modest: 5 to 8 W at 1064 nm for P1, and 500 mW or less at 532 nm for P2 and P3. However, the fast beam scanning means the pulse repetition rate has to be very high (up to 100 kHz) in order to achieve the desired pulse overlap (see Figure 8). Q-switched diode-pumped solid state (DPSS) infrared and green lasers are designed specifically to deliver this combination of performance, as well as short (<30 nanoseconds) pulse duration.

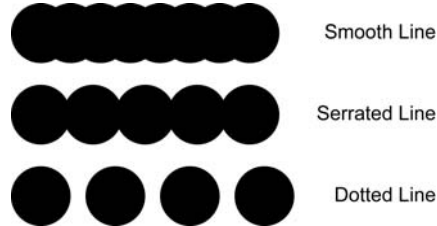


Fig. 8. A high pulse repetition rate is necessary to deliver a continuous cut with desired pulse overlap. The serrated geometry is desired in order to eliminate layer peel associated with smooth scribe lines and to minimize re-cast ridges.

4.2. Short Pulsewidths for Minimum HAZ

Q-switched DPSS lasers can deliver pulsewidths ranging from 10 ns to over 100 ns. For these scribing applications, a short pulsewidth is desirable since this produces the cleanest edges and smallest HAZ (see Figs. 5-7). Edge damage and other HAZ effects are caused in part by cumulative thermal loading which is therefore minimized with short pulses having high peak power. But in all Q-switched lasers there is a trade-off between output parameters such as pulse width, repetition rate and average power at any given cavity length. Specifically, increasing the repetition rate increases the pulsewidth. However, optimized DPSS lasers are able to deliver the requisite combination of high (100 kHz) repetition rate *and* short (< 30 ns) pulsewidth by use of a specially designed short cavity. (Note: the use of sub-ns – or so-called ‘ultrafast’ lasers – is not suited for this application, due to both their significantly higher unit cost compared to nanosecond lasers and the limited process benefits obtained when, for example, moving from ns to ps.)

4.3. Beam Pointing Stability

Q-switched DPSS lasers optimized for thin-film PV scribing are also designed to deliver superior pointing stability, even under demanding 24/7 operating conditions and changing ambient temperatures. Their industry-leading specification has been achieved by a combination of inherent passive stability in the unique cavity design supported by active stabilization loops. Extreme pointing stability is necessary to enable narrower scribe lines with closer spacing in Gen 8.5 panels, since larger panels involve longer optical beam delivery paths than ever before in this application, amplifying any drifts in beam pointing direction.

4.4. Beam Quality and Output Stability

Another key characteristic of these solar scribing optimized lasers is the combination of beam quality and output mode stability. Q-switched DPSS lasers are designed to deliver a single transverse mode, i.e., a TEM₀₀ beam with a Gaussian cross-section, in contrast to alternative multi-mode lasers. Moreover, the cavity stability ensures that following the start-up phase, the laser continues to produce this same Gaussian output. This type of output delivers superior scribe edges. In addition, the mode stability means that the cut width and cut quality are constant.

High pulse-to-pulse energy stability is a critical factor because the scribe width is dependent on pulse energy; fluctuations in this energy can deliver inconsistent cuts. Due to the low pulse overlap employed in the scribing process, variation in ablated spot size, D , can lead to process failure. For example, when using a 25% overlap, if the size of the spot shrinks by 25% *for any single pulse*, the pulses will lose their connectivity (the “dotted line” of Fig. 8) and adjacent cells will not be isolated (P1 and P3). In Figure 9, we plot normalized spot size as a function of pulse energy for all three scribing steps. Here, we (conservatively) specify process breakdown when the normalized spot size, D/D_0 , falls below 80%.

For the P1 step (Fig. 9a), the pulse energy, E , can fall to about 75% of its nominal value, E_0 , before the spot size shrinks below 80% of its nominal value. For the P2 step (Fig. 9a), D/D_0 hits 80% when the pulse energy falls to about 67% of its nominal value. Similarly for P3, process breakdown occurs when $E/E_0 \approx 66\%$ (Fig. 9c).

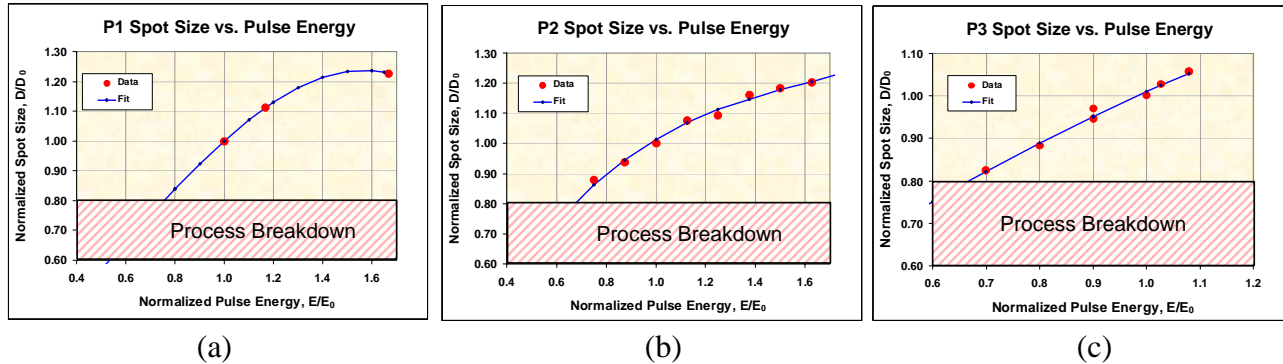


Fig. 9. Dependence of focused spot size (scribe width) on laser pulse energy for (a) P1, (b) P2, and (c) P3 process steps.

These data suggest that for scribing thin-film PV panels, the key requirement for laser pulse stability is somewhat different from other applications. The process has plenty of latitude with respect to fluctuations in pulse energy. So keeping pulse-to-pulse energy fluctuations within a tight band is not so critical. However, the pulse energy must remain steady over tens or hundreds of billions of pulses (a single scribe across a Gen 8.5 panel may contain up to 10^5 pulses). Consequently, a 3-sigma specification on pulse stability is relatively meaningless. Rather, a specification that stipulates part-per-billion levels of the occurrence of “runt” pulses (e.g., $E < 0.70E_0$) is more appropriate. For Gen 8.5 panels, each scribe pattern (P1, P2, and P3) will require over 10^7 laser pulses. To keep manufacturing yield losses in the scribing step to less than 0.01%, the laser must produce no runt pulses over an operating period containing on the order of 100 billion pulses.

To explore the capability of our optimized laser to meet this requirement, a long-duration test was designed to detect runt pulses. Using a digitizing oscilloscope (Tektronix model TDS7054), the laser was run 24/7 for one week and the scope was set up to trigger if the amplitude of any single pulse fell below 70% of the mean amplitude (see Figure 10). During this test, no oscilloscope trigger events occurred. To confirm test fidelity, the trigger was checked by blocking the beam at three points during the experiment: the start of the test, after five days of operation, and at the end of the run. In practical terms, this test translates to a 50 part-per-trillion failure level with 95% confidence level or 100 parts per trillion at 99.7% confidence level.

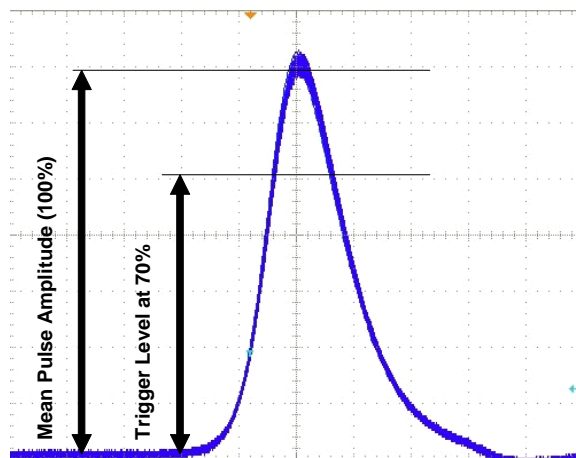


Fig. 10. Test scheme to detect runt pulses in optimized Q-switched DPSS scribing laser. Laser output: 1064nm wavelength, 16W power at 100 kHz pulse repetition frequency.

4.5. Reliability and Downtime

From a practical standpoint, the importance of laser reliability cannot be overstated. Thin-film solar panels are commodity products where even high-volume manufacturing delivers only modest margins. These margins can be reduced even further by unscheduled downtime. Moreover, with three scribe stations each using multiple lasers, if just one of these lasers stops delivering specified performance, the entire production line must be stopped until the problem is rectified. All aspects of DPSS laser design and manufacturing should therefore be thoroughly optimized to deliver high reliability and long operating lifetimes, from the component level optics mounts and pump diodes, through cavity design and cleanroom assembly methods, to extensive testing and final certification. Just as important, these lasers are also designed for fast field maintenance. For example, the main consumables are the pump diode arrays, which now deliver over 10,000 hours thanks to the use of AAA (aluminum-free active area) diode technology. An architecture permitting easy field serviceability locates the fiber-coupled (FAP) pump diode array in a separate compartment so that it can be replaced in the field in just a few minutes with no need for laser re-alignment and without disturbing the beam pointing of the laser output.

5. CONCLUSION

Successful widespread use of solar energy in commercial, government and residential markets requires up to a three-fold reduction in manufacturing costs while maximizing the conversion efficiency of the final modules. The advent of next generation thin-film solar technology is an important step along the road to grid cost parity. Laser scribing is poised to play a key role in enabling this step to occur. Solar cell manufacturing is a demanding application for lasers because it both requires high precision and is extremely cost sensitive. The particular combination of economic and technical constraints encountered in thin-film photovoltaic manufacturing thus differs from that of many other current laser applications. This challenge can be met by utilizing a laser whose output has been specifically optimized for the needs of the process, and which has been designed and constructed to deliver a very high level of operational consistency and reliability.

6. REFERENCES

1. P. Maycock, "2006-2015 World PV Market: Technology and Cost," PV Energy Systems, 2007.
2. Ibid.
3. Ibid.
4. C. Dunskey, "Lasers in the solar energy revolution," *Industrial Laser Solutions*, Vol. 22, No. 8, August 2007, pp. 24-27.
5. P. Grunewald, "Laser Processing Technologies for Thin-Film Solar Cells," Japan Laser Processing Society, December 2007, Proceedings of the 69th Laser Materials Processing Conference, pp 91-85.
6. C. Dunskey and F. Colville, "Laser scribing of thin-film solar panels," *Industrial Laser Solutions*, Vol. 23, No. 2, February 2008, *to appear*.
7. Maycock, 2007
8. S. Haas, A. Gordijn, H. Stiebig, "Influence of the laser parameters on the patterning quality of thinfilm silicon modules," SPIE Optics and Photonics, August 2007. Proceedings of SPIE Vol. 6651, Paper 16